Flashing Superluminal Components in the Jet of the Radio Galaxy 3C120

José-Luis Gómez,[1*] Alan P. Marscher,[2] Antonio Alberdi,[1] Svetlana G. Jorstad,[2,3†] Cristina García-Miró[1]

A 16-month sequence of radio images of the active galaxy 3C120 with the Very Long Baseline Array reveals a region in the relativistic jet where superluminal components flash on and off over time scales of months, while the polarization angle rotates. This can be explained by interaction between the jet and an interstellar cloud located about 8 parsecs from the center of the galaxy. The cloud, which rotates the polarization direction and possibly eclipses a section of the jet, represents a "missing link" between the ultradense broad–emission-line clouds closer to the center and the lower density narrow–emission-line clouds seen on kiloparsec scales.

Relativistic jets, which are presumably byproducts of the accretion of gas onto supermassive central black holes (*1*, *2*), are commonly observed in active galactic nuclei (AGNs). Broad (corresponding to motions of thousands of kilometers per second emission lines from very dense (on the order of 10^{10} electrons cm^{-3}) clouds are commonly observed close to the "central engines" of AGNs, together with somewhat narrower lines from less dense (on the order of 10^3 to 10^4 electrons cm^{-3}) clouds located hundreds or thousands of parsecs farther out (*3*). It has remained unclear whether these clouds represent matter that is flowing out of, falling into, rotating around, or engaged in random motions about the central black hole. Observations of clouds at intermediate ranges would help to resolve this issue.

Very long baseline interferometry (VLBI) observations at high radio frequencies (22 and 43 GHz) can produce images of the jets in AGNs with resolutions ranging from 0.1 to 0.3 milliarcsecond (mas), which correspond to linear scales as small as about 0.1 pc in relatively nearby (100 to 200 Mpc) powerful AGNs. One of the best candidates for such a study is the radio galaxy 3C120 [redshift $z = 0.033$ (*4*), placing it at a distance of $\sim 140\ h_{65}^{-1}$ Mpc, where h_{65} is the Hubble constant in units of 65 km s^{-1} Mpc^{-1}], which is among the first objects in which superluminal motion was detected (*5*, *6*). Here we report monthly polarimetric Very Long Baseline Array (VLBA) observations of 3C120 at 22 and 43 GHz over 16 epochs that allow us to study, with the finest linear resolution available ($0.2\ h_{65}^{-1}$ pc) (*7*, *8*), the inner magnetic field structure and the evolution of bright features ("components") as they propagate down the jet at apparent superluminal speeds.

The VLBA images (Fig. 1) show a richer, more rapidly changing structure in total and linearly polarized intensity than that found in other relatively nearby compact extragalactic jets (*9*–*11*). An animation generated through the combination of the 16 total and polarized intensity images of Fig. 1 can be viewed and downloaded at *Science* Online (www.sciencemag.org/feature/data/1052657.shl). Multiple components can be distinguished in the images (Fig. 1), with apparent motions between 4 and 6 $h_{65}^{-1}\ c$ (c is the speed of light) relative to the unpolarized core, which lies at the eastern (upstream) end of the jet and is presumed to be stationary. The structure of the inner 2 mas in the jet is dominated by the appearance of a new superluminal (apparent velocity of $4.4\ h_{65}^{-1}\ c$) component (labeled *O* in Fig. 1), associated with a major outburst [from ~ 3 to a peak of ~ 6 jansky (Jy; 1 Jy = 10^{-26} W m^{-2} Hz^{-1}) in April 1998] in the radio flux of 3C120 (*12*). The passage of this new component across a stationary component (M, 0.8 mas from the core) caused the polarization of both components to increase.

From the observed maximum proper motion of 6 $h_{65}^{-1}\ c$, we can estimate an upper limit to the viewing angle (*13*) of $\sim 20°$ and a minimum Lorentz factor [for the pattern speed (*14*) of the components] of 6. The observed jet opening angle of 5° translates in the source frame to $\leq 1.7°$ (for a viewing angle of $\leq 20°$), which is consistent with a well-collimated jet in 3C120.

We resolve the jet across its width in the outer 2 to 8 mas (Fig. 2) and find that the components do not fill the entire jet width. Rather, they are ejected along different position angles and travel along different, gently curved paths. (The curvature is amplified by projection effects because the jet is viewed within 20° of end-on.) This supports the idea that the bright components are created by perturbations in the flow velocity or energy flux, leading to the formation of shock waves (*15*) that are restricted to regions smaller than the jet width.

Between about 2 and 4 mas west of the core there is an asymmetry across the jet width. Two different types of components can be distinguished: those lying on the northern side and those on the southern side of the jet axis (Fig. 2). Northern components commonly contain magnetic polarization vectors oblique to the axis but constant in orientation, whereas southern components have magnetic polarization vectors whose directions rotate as the components travel downstream, with the vectors eventually becoming perpendicular to the components' velocity vectors.

The light curves of the individual features (Fig. 3) reveal a remarkable brightening of components (especially the southern ones), starting at a distance from the core of ~ 2 mas. The most pronounced (in terms of change in flux density) flare corresponded to component L, which increased its total flux density by a factor of 9 (from 50 to 450 mJy), thereafter momentarily (on 3 December 1998) becoming the strongest feature in polarized intensity (Fig. 1). This flare was accompanied by a rotation of the magnetic vector by about 140° (Fig. 3) and an increase in degree of polarization from 12 to 18%. A similar flare in total and polarized flux density was also observed at 43 GHz, during which the degree of polarization increased from 7 to 17% while the magnetic vector rotated by 43° (Fig. 3). This slower rotation of the magnetic vector at 43 GHz reveals a progressive increase in the rotation measure (RM) of component L, reaching a value of $\sim 6000 \pm 2400$ rad m^{-2} at peak emission (December 1998). Component H underwent a similar flare and probably a similar rotation of the field, although we can distinguish its polarization from component J only after the 7 February 1998 epoch, when it was observed to have a magnetic vector perpendicular to the component's motion.

The rapid flares in the flux densities of components H and L were followed by equally fast declines when they reached ~ 3 mas from the core. Component H was observed to decrease its flux density so much that it appeared to be blended with the outer contours of component J between September and December 1998. By January 1999,

[1]Instituto de Astrofísica de Andalucía (CSIC), Apartado 3004, Granada 18080, Spain. [2]Institute for Astrophysical Research, Boston University, 725 Commonwealth Avenue, Boston, MA 02215, USA. [3]Astronomical Institute, St. Petersburg State University, Bibliotechnaya Ploschad' 2, Petrodvoretz, St. Petersburg 198904, Russia.

*To whom correspondence should be addressed. E-mail: jlgomez@iaa.es
†Formerly S. G. Marchenko.

component H could once again be distinguished from J, emerging at the extrapolated position based on its previous proper motion (Fig. 2), with a similar orientation of its magnetic vector.

It is difficult to explain such rapid changes in the total and polarized flux density, as well as polarization angle, for components located between a deprojected distance of 4 and 10 pc from the core. The bending of the jet appears to be too slight to cause such variations in brightness (from changing relativistic beaming of the radiation relative to the observer) without an accompanying acceleration of the apparent velocity and the presence of a stationary component at this site (*16*, *17*). Rather, interaction between the jet and a dense cloud in the external medium seems the most plausible explanation. Similar interactions between the jet and the interstellar medium were inferred previously from the discovery of an emission line counterpart to the more extended radio jet in 3C120 (*18*, *19*). It appears that this interaction is most intense along the southern border of the jet, where the gentle northward curvature causes components with higher than average momentum to collide with the external medium or cloud. It is at the beginning of this bend that component L, which is the closest to the southern jet border and the one exhibiting the largest flare, began to increase its flux density. This behavior is explained if the magnetic field and population of relativistic electrons in component L are enhanced by the shock wave produced by the interaction of the jet with the external medium, resulting in a rapid rise in synchrotron emission. The observed increase in the degree of polarization is then explained as a consequence of ordering of the field by the shock wave. The rotation of the magnetic vector observed in component L can be interpreted as Faraday rotation (*20*), the level of which can be estimated from the different polarization angles observed at 22 and 43 GHz (Fig. 3). After removing this effect, the relative orientation of the magnetic field and velocity vector (which rotates as the component follows the bend in the jet) remains at 40° ± 10°, in good agreement with the orientation of 35° ± 10° observed for component D, which appears to be a more evolved version of component H.

The observed Faraday rotation can be explained by an ionized cloud along the line of sight that may also physically interact with the jet. This cloud should also cause free-free absorption of the jet emission; its location can then be revealed by studying the spectral index distribution of the jet (Fig. 4), yielding a deprojected distance (for a viewing angle of 20°) of ~8 pc from the center of the galaxy.

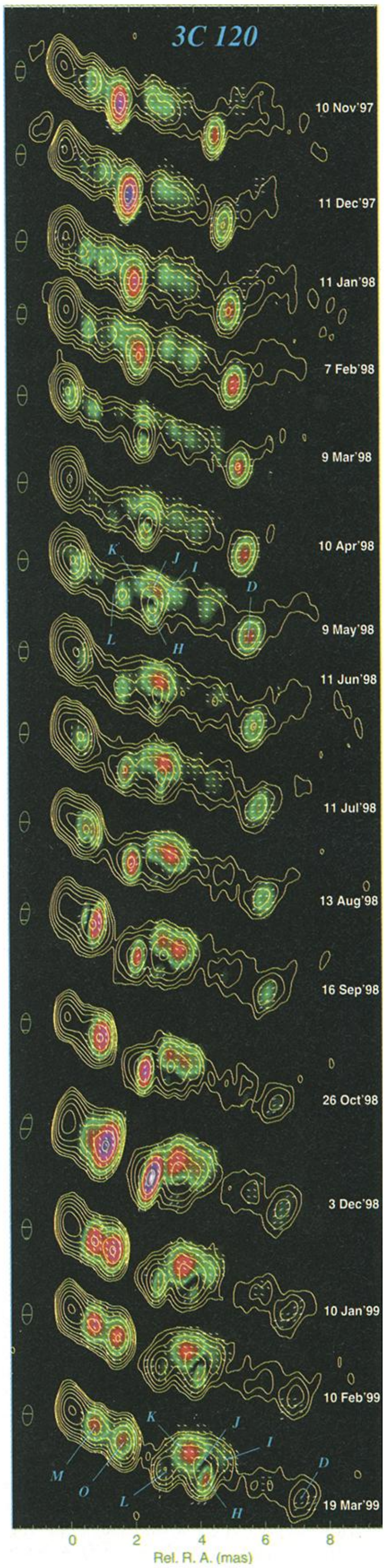

Fig. 1. VLBI images of 3C120 at 22.22 GHz (*27*). Observing epochs are indicated at the right of each image. Vertical image separation is proportional to the time differences of the epochs of observation. Contours give the total intensity; colors (on a linear scale from green to white) show the polarized intensity; and bars (of unit length) indicate the direction of the magnetic polarization vector. Synthesized beams are plotted at the left of each image, with a typical size of 0.6 × 0.3 mas (0.3 mas corresponds to 0.2 h_{65}^{-1} pc). The root mean square (rms) noise (peak of brightness) in polarization corresponds to 1.5 mJy per beam (52.4 mJy per beam). Seven logarithmic contours are plotted for each total intensity image between the rms noise (typically ~2 mJy per beam) and 90% of the peak of brightness. Rel. R.A., relative right ascension.

Assuming an intrinsic spectral index between 22 and 43 GHz of $\alpha = -0.8$, we obtain a lower limit for the cloud free-free opacity at 22 GHz of $\tau_{ff} \geq 0.4$. Free-free opacity is given by (*21*) $\tau_{ff} = 9.8 \times 10^{-3}\, l\, n_e^2\, T^{-1.5}\, \nu^{-2}\, [17.7 + \ln (T^{1.5}\, \nu^{-1})]$, where l is the column length, n_e is the electron density, T is the temperature, and ν is the frequency. For a cloud at $T = 10^4$ and a column length $l \sim 0.4$ pc (estimated from Fig. 4), free-free absorption would provide the required opacity for an electron density $n_e \geq 4.6 \times 10^4$ cm^{-3}. The observed RM of ~6000 ± 2400 rad m^{-2} would then require a magnetic field strength $B_{\parallel} \leq 0.4$ μG. Similarly large RMs have been found in several extragalactic jets (*22*, *23*), with estimated magnetic fields of the same order.

This electron density and distance from the central engine are intermediate between those of the broad and narrow (actually, less broad) emission-line clouds in AGNs. Given its high column density (~6 × 10^{22} cm^{-2}), such a cloud could easily be detected in absorption if there were a substantial neutral atomic or molecular component, as expected. Such an observation, which could be carried out with the VLBA in spectral-line mode, would determine the radial velocity of the cloud and therefore whether it is moving toward or away from the central engine.

Although rapid increases in brightness can result from the interaction of components with a dense cloud, it is in general difficult to reproduce the rapid decays observed in components H and L (Fig. 3) as fast as d^{-11} (here, d is the component's size). The general expansion of the jet is too gradual to produce such a steep decline in flux density, and the radiative energy losses of the electrons are too weak this far down the jet. For the equipartition magnetic field B, the synchrotron cooling time scale in the plasma rest frame is given by (*24*) $t_{syn} \approx 1.38 \times 10^{12}\, \delta^{(4\alpha+9)/[2(\alpha+3)]}\, B^{-3/2}\, \nu^{-1/2}$ s, where δ is the Doppler factor. From the observed apparent motions we estimate $\delta \sim 3$, which, for an observed cooling time scale of 1 month and $\alpha \sim -0.8$, leads to $B \geq 20$ G. This is higher than the value of $\sim$0.01 G (to within a factor of 10) expected on parsec scales, from which we conclude that synchrotron plus adiabatic cooling alone cannot account for the rapid decay in flux density of components L and H.

The flashing of component H could be due to either the passing of the component through a jet rarefaction or partial occultation by the foreground absorbing cloud. Because the radio spectrum does not show evidence for large opacities when H is observed to merge with component J, the cloud must have a sharp edge at which it becomes opaque at 43 GHz; this would require an increase of the cloud density to values on the order of 2×10^5 cm^{-3}.

Bending of the jet in the 2- to 4-mas region should lead to the formation of standing compression and rarefaction waves in the jet fluid (*25*). Moving components would then be expected to show a rise and fall in their flux density when passing through this structure. The lack of a bright stationary feature in this region is perplexing in this context, because it suggests that the compression wave might not be strong enough to produce the flashing of components H and L. (It could more easily explain the rise in flux density in the northern components; these might also be affected by weak interaction with the external medium, which would account for their oblique polarization.) The interaction of the jet with the external medium may therefore be a dynamic rather than steady-state process, perhaps owing to small changes in the direction of the jet "nozzle." The theoretical reproduction of such phenomena and the study of jet-cloud collisions remain a challenge for three-dimensional relativistic hydrodynamical jet simulations (*2*, *26*).

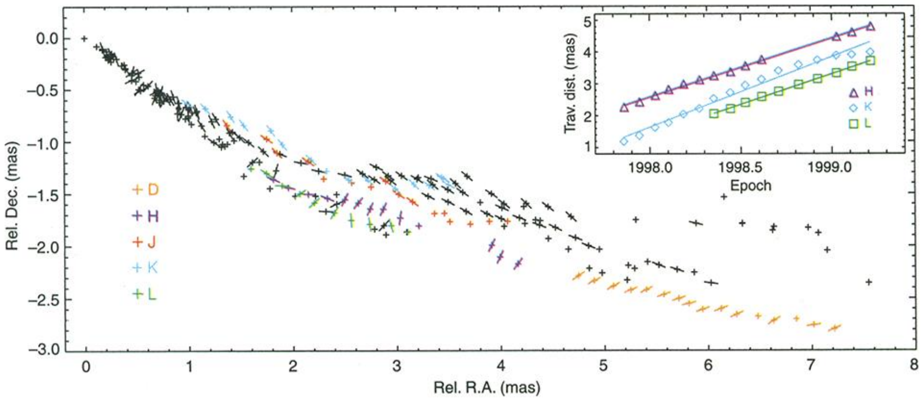

Fig. 2. Positions and magnetic vector orientations of the components obtained from Gaussian model fitting of the images shown in Fig. 1. Components D, H, J, K, and L are identified with different colors. The inset shows the traveled distance (separation from the core) as a function of time for components H, K, and L. Rel. Dec., relative declination.

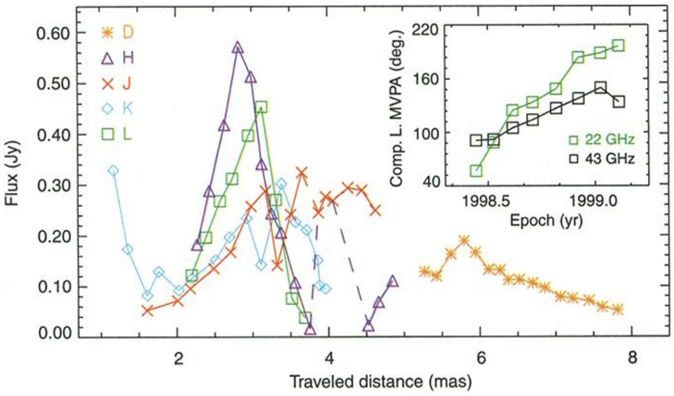

Fig. 3. Evolution of flux density as a function of the distance from the core for components D, H, J, K, and L. Component H cannot be distinguished from J between 3.7 and 4.5 mas from the core. The inset shows the evolution with time of the magnetic vector position angle of component L.

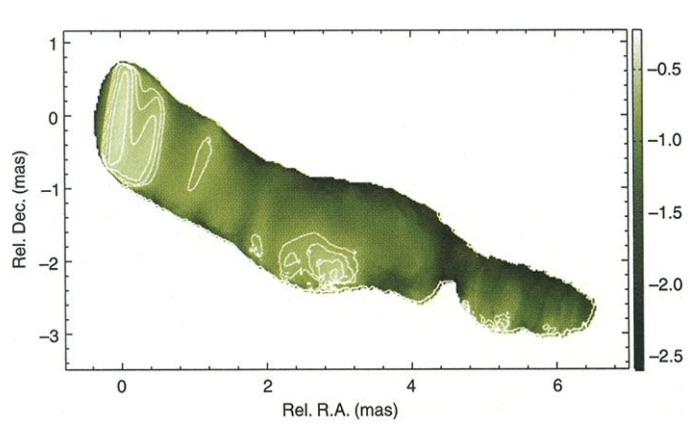

Fig. 4. Spectral index (α, where flux density $S_\nu \propto \nu^\alpha$) map between 22 and 43 GHz, obtained by adding the images of all 16 epochs using a common convolving beam for both frequencies of 0.62×0.3 mas at a position angle of $-3°$. Contours are shown for $\alpha = -0.6, -0.5, -0.4$, and -0.3.

References and Notes

1. R. Ouyed, R. E. Pudritz, J. M. Stone, *Nature* **385**, 409 (1997).
2. S. Koide, K. Shibata, T. Kudoh, *Astrophys. J.* **522**, 727 (1999).
3. H. Netzer, in *Active Galactic Nuclei*, T. J.-L. Courvoisier and M. Mayor, Eds. (Springer-Verlag, New York, 1990), p. 67.
4. E. M. Burbidge, *Astrophys. J.* **149**, L51 (1967).
5. G. A. Seielstad *et al.*, *Astrophys. J.* **229**, 53 (1979).
6. R. C. Walker, J. M. Benson, S. C. Unwin, *Astrophys. J.* **316**, 546 (1987).
7. J. L. Gómez, A. P. Marscher, A. Alberdi, J. M. Martí, J. M. Ibáñez, *Astrophys. J.* **499**, 221 (1998).
8. J. L. Gómez, A. P. Marscher, A. Alberdi, *Astrophys. J.* **521**, L29 (1999).
9. W. Junor, J. A. Biretta, M. Livio, *Nature* **401**, 891 (1999).
10. S. J. Tingay *et al.*, *Astron. J.* **115**, 960 (1998).
11. K. I. Kellermann, R. C. Vermeulen, J. A. Zensus, M. H. Cohen, *Astron. J.* **115**, 1295 (1998).
12. The outburst in the flux was observed with Metsähovi flux density monitoring at 22 GHz (H. Teräsranta, personal communication).
13. The viewing angle is defined as the projection angle through which the jet is seen by the observer.
14. Pattern speed refers to the velocity of the fluid perturbation identified with the component; this may differ from the actual velocity of the fluid in the component.
15. J. L. Gómez, J. M. Martí, A. P. Marscher, J. M. Ibáñez, A. Alberdi, *Astrophys. J.* **482**, L33 (1997).
16. A. Alberdi *et al.*, *Astrophys. J.* **402**, 160 (1993).
17. J. L. Gómez, A. Alberdi, J. M. Marcaide, A. P. Marscher, J. P. Travis, *Astron. Astrophys.* **292**, 33 (1994).
18. D. J. Axon *et al.*, *Nature* **341**, 631 (1989).
19. C. T. Hua, *Astron. Astrophys.* **199**, 105 (1998).
20. Faraday rotation of linearly polarized radio waves occurs when the radiation passes through an electron-proton plasma containing a magnetic field. The effect is inversely proportional to the square of the frequency.
21. A. P. Marscher and R. L. Brown, *Astrophys. J.* **200**, 719 (1975).
22. P. S. Udomprasert, G. B. Taylor, T. J. Pearson, D. H. Roberts, *Astrophys. J.* **483**, L9 (1997).
23. G. B. Taylor, *Astrophys. J.* **506**, 637 (1998).
24. G. V. Bicknell and M. C. Begelman, *Astrophys. J.* **467**, 597 (1996).
25. V. Icke, in *Beams and Jets in Astrophysics*, P. A. Hughes, Ed. (Cambridge Astrophysics Series, Cambridge, 1991), pp. 238–261.
26. M. A. Aloy, J. L. Gómez, J. M. Ibáñez, J. M. Martí, E. Müller, *Astrophys. J.* **528**, L85 (2000).
27. Observations were obtained with the 10 antennas of the VLBA. The data were recorded in 1-bit sampling VLBA format with 32-MHz bandwidth per circular polarization. The reduction of the data was performed with the AIPS software in the usual manner [K. J. Leppänen, J. A. Zensus, P. J. Diamond, *Astron. J.* **110**, 2479 (1995)]. The absolute phase offset between right- and left-circular polarization at the reference antenna was determined by comparison with 14 Very Large Array (VLA) observa-

tions at the following epochs: 21 November 1997, 14 December 1997, 15 January 1998, 12 February 1998, 7 March 1998, 8 April 1998, 9 June 1998, 11 July 1998, 14 August 1998, 19 September 1998, 29 October 1998, 28 November 1998, 17 February 1999, and 17 March 1999. The calibrator sources 0420-014, OJ287, BL Lac, and 3C454.3 were used to compare the VLA and VLBA integrated polarization position angles. Estimated errors in the orientation of the magnetic vectors vary from epoch to epoch, but usually lie in the range of 5° to 10°. Simultaneous observations at 43 GHz were also obtained for all observing epochs, with an estimated error in the orientation of the magnetic vectors between 7° and 15°.

28. Supported in part by the Spanish Dirección General de Investigación Científica y Técnica under grant PB97-1164, by the U.S. NSF through grant AST-9802941, and by the Fulbright commission for collaboration between Spain and the United States. We thank J. M. Martí for comments on our manuscript. The VLBA is an instrument of the National Radio Astronomy Observatory, a facility of the U.S. NSF operated under cooperative agreement by Associated Universities Inc.

30 May 2000; accepted 3 August 2000

Quantum Hall Ferromagnetism in a Two-Dimensional Electron System

J. Eom,[1] H. Cho,[1] W. Kang,[1*] K. L. Campman,[2] A. C. Gossard,[2] M. Bichler,[3] W. Wegscheider[3,4]

Experiments on a nearly spin degenerate two-dimensional electron system reveals unusual hysteretic and relaxational transport in the fractional quantum Hall effect regime. The transition between the spin-polarized (with fill fraction ν = 1/3) and spin-unpolarized (ν = 2/5) states is accompanied by a complicated series of hysteresis loops reminiscent of a classical ferromagnet. In correlation with the hysteresis, magnetoresistance can either grow or decay logarithmically in time with remarkable persistence and does not saturate. In contrast to the established models of relaxation, the relaxation rate exhibits an anomalous divergence as temperature is reduced. These results indicate the presence of novel two-dimensional ferromagnetism with a complicated magnetic domain dynamic.

The two-dimensional electron system (2DES) under low temperatures and high magnetic fields has become a test bed for studying quantum phase transitions in low dimensions (*1–3*). Unlike classical phase transitions that are driven largely by thermal fluctuations, the phase transitions found in the quantum Hall effect (QHE) regime represent a class of zero temperature phase transitions that are driven by strong electron-electron interaction. Under intense magnetic fields, quantization of the electronic motion into Landau levels quenches the kinetic energy and the interaction energy determines the thermodynamic properties of the underlying 2DES. At integral and certain fractional commensuration of the electron density and the applied magnetic flux, called filling fraction ν, gain in the interaction energy produces transitions to the quantum Hall states with Hall conductance $\sigma_{xy} = \nu e^2/h$ (*1*, *2*). The collective, many-body nature of the QHE states is evident from the dissipationless longitudinal transport and the existence of energy gap in the excitation spectrum. The magnetotransport in the vicinity of a transition between two QHE phases is well described in terms of critical behavior normally associated with a second-order phase transition. The universal scaling exhibited by the QHE transitions and the existence of well-defined critical exponents provide compelling evidence indicative of a zero-temperature quantum phase transition (*3–5*).

In addition to the transitions between two different QHE states, the translationally invariant quantum Hall phases can exhibit novel forms of two-dimensional ferromagnetism (*6*). Driven by gain in the anisotropy energy over the Coulomb exchange energy, the ferromagnetic transitions in the multicomponent QHE systems are accompanied by spatial ordering of pseudospin degrees of freedom represented by discrete quantum numbers such as electronic spin, Landau level index, and electron layer quantum number. Analogous to the ferromagnetically ordered electronic spins in magnetic systems, resulting quantum Hall ferromagnets represent a new class of low-dimensional ferromagnets with remarkable properties (*7*, *8*). The distinguishing features of quantum Hall ferromagnets include broken symmetry arising from spontaneous magnetic ordering, existence of Goldstone mode in the ordered state, and topological objects as its low-energy excitations (*6*).

The underlying symmetry of the quantum Hall ferromagnet is determined by the associated pseudospin of the QHE phase. In case of even integral QHE states in single-layer electron systems, the spin configuration of the associated Hall states becomes the pseudospin quantum number of the transformed state. Because the possible spin geometries are limited to a fully polarized state with all electron spins aligned parallel to the applied magnetic field and an unpolarized state with equal numbers of up and down spins, the resulting pseudospin degree of freedom possesses a bimodal, Ising symmetry. In double-layer 2DESs found in double quantum wells or a wide quantum well, the in-plane degree of freedom leads to a transition to a two-dimensional XY ferromagnet (*9–11*). In some QHE states, interplay of spin and the layer quantum numbers can produce a transition to an Ising ferromagnet in wide-well system (*8*, *12*).

Our experiment was performed on a high-quality GaAs/AlGaAs heterostructure. Data was taken at pressures above 10 kbar where a large reduction in the magnitude of the electronic *g* factor favors formation of spin-unpolarized fractional quantum Hall effect (FQHE) states. The evolution of the ν = 2/5 FQHE state with pressure indicates enhancement of spin fluctuations against their tendency to align parallel to the applied magnetic field. Under increasing pressure, the spin-unpolarized ground state competes against the spin-polarized state, leading to coexistence over a broad region of pressure. The transition to the pseudospin ferromagnetic state is distinguished by emergence of hysteretic transport and anomalous temporal relaxation of magnetoresistance. The observed correlation between hysteretic and relaxational evolution of magnetotransport points toward existence of intriguing domain dynamics in the pseudospin ferromagnet.

The density of the GaAs/AlGaAs heterostructure used in the experiment was $n = 3.5 \times 10^{11}$ cm^{-2} with mobility of $\mu = 2.4 \times 10^6$ cm^2/V s. A miniature beryllium-copper pressure cell was used to achieve high pressure. Samples were immersed inside a homogeneous hydrostatic medium that transmits uniform pressure to the sample. A small light-emitting diode was placed inside the pressure cell to illuminate the sample at low temperatures. A gradual reduction in the electronic density was found with increasing pressure.

The magnetoresistivity of a high-quality 2DES sample is shown (Fig. 1) in the hysteretic region found between 11 to 14 kbar of

[1]James Franck Institute and Department of Physics, University of Chicago, Chicago, IL 60637, USA. [2]Department of Electrical Engineering, University of California at Santa Barbara, Santa Barbara, CA 93106, USA. [3]Walter Schottky Institut, Technische Universität München, Am Coulombwall, D-85748 Garching, Germany. [4]University of Regensburg, Regensburg, Germany.

*To whom correspondence should be addressed. E-mail: wkang@midway.uchicago.edu